

Supporting information

Structure and dynamics of micelle-associated human immunodeficiency virus gp41 fusion domain

Christopher P. Jaroniec, Joshua D. Kaufman, Stephen J. Stahl,
Mathias Viard, Robert Blumenthal, Paul T. Wingfield, and Ad Bax

Table S1. Resonance assignments for HIV-1 gp41 fusion domain in SDS micelles.

Residue	$^1\text{H}^\alpha$ (ppm)	$^1\text{H}^N$ (ppm)	^{15}N (ppm)	$^{13}\text{C}^\beta$ (ppm)	$^{13}\text{C}^\alpha$ (ppm)	$^{13}\text{C}^\beta$ (ppm)
Pro	—	—	—	172.148	62.223	31.404
A1	4.408	8.637	123.301	177.320	52.819	18.259
V2	4.135	7.803	116.292	176.322	61.922	32.089
G3	4.038/4.097	8.245	110.332	175.451	45.521	—
I4	3.936	8.015	120.517	177.059	62.952	37.030
G5	3.758/3.953	8.494	108.814	174.924	47.267	—
A6	4.124	7.858	122.321	181.229	54.374	17.467
L7	4.129	7.894	119.852	179.276	57.254	41.014
F8	4.362	8.321	118.961	177.364	60.597	38.619
L9	4.002	8.520	118.128	180.452	57.545	40.317
G10	3.886/3.924	8.152	107.337	176.476	46.330	—
F11	4.454	8.010	122.887	177.294	59.964	38.477
L12	3.869	8.163	118.931	179.148	56.958	40.738
G13	3.897	8.122	105.416	175.794	46.122	—
A14	4.305	7.813	124.130	179.265	53.241	17.991
A15	4.115	8.186	121.774	179.144	53.665	17.644
G16	3.856/3.956	8.355	105.730	175.454	46.140	—
S17	4.433	7.994	115.200	175.969	59.597	63.366
T18	4.275	8.014	115.913	175.459	63.385	68.909
M19	4.395	8.155	120.431	177.194	56.458	31.981
G20	3.942/3.988	8.215	108.005	174.894	45.662	—
A21	4.290	7.996	123.097	178.345	52.970	18.236
A22	4.288	8.094	120.976	178.229	52.951	18.129
S23	4.375	8.082	113.138	174.938	58.832	63.425
M24	4.500	8.017	121.011	176.217	55.836	32.229
T25	4.335	8.050	114.237	174.454	61.941	69.373
L26	4.413	8.042	123.240	177.147	55.082	41.522
T27	4.367	8.018	114.224	174.483	61.531	69.461
V28	4.123	8.003	121.688	176.087	62.031	31.831
Q29	4.311	8.332	123.233	175.681	55.351	28.649
A30	4.262	8.242	125.146	177.245	52.132	18.607
D31	4.564	8.242	119.349	175.823	53.780	40.526
Y32	4.504	8.038	120.690	175.530	57.737	38.178
K33	4.281	8.027	123.475	175.733	55.394	32.560
D34	4.560	8.281	121.909	176.055	53.904	40.791
D35	4.581	8.306	120.771	176.181	54.119	40.637
D36	4.591	8.325	120.319	176.065	54.296	40.637
D37	4.628	8.297	120.557	175.234	53.947	40.309
K38	4.142	7.713	126.019	—	57.197	32.752

Assignments were obtained at 25 °C and 600 MHz ^1H frequency using 3D HNCO, HNCA, HN(CA)CB, and ^1H - ^{15}N TOCSY-HSQC experiments recorded on 0.7 mM ^{13}C , ^{15}N , ^2H - and ^{15}N -labeled samples (see main text). Differences in $^1\text{H}^N$ shifts between the ^{13}C , ^{15}N , ^2H - and ^{15}N -labeled samples were ≤ 0.01 ppm.

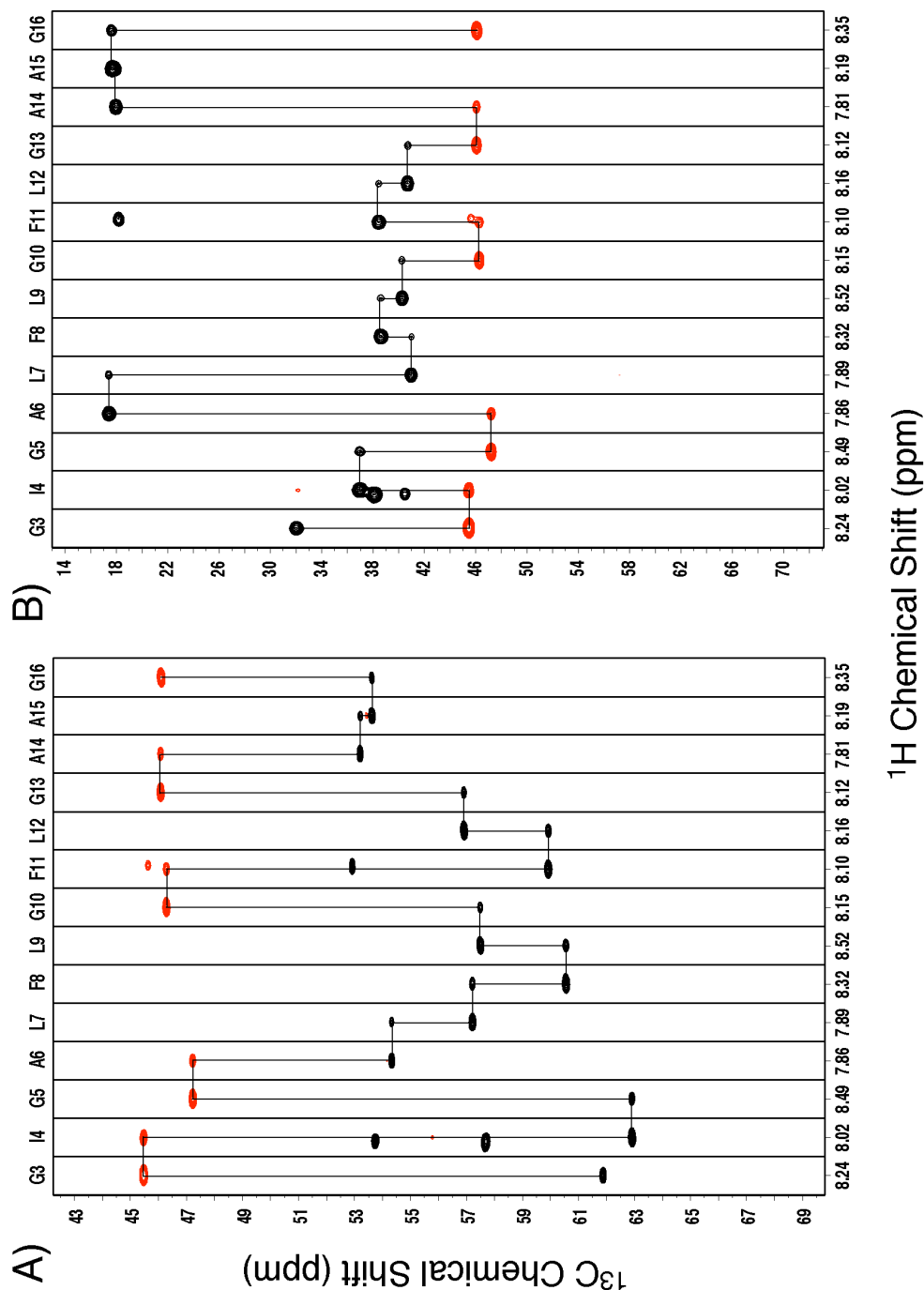


Figure S1. Representative strips from 600 MHz 3D CT-HNCA (a) and HN(CA)CB (b) spectra (I) of HIV-1 gp41 fusion domain. (a) 3D CT-HNCA: spectrum was recorded as a $100^* \times 40^* \times 440^*$ data matrix with acquisitions times of 24 ms (t_1 , ^{13}C), 24 ms (t_2 , ^{15}N) and 54 ms (t_3 , ^1H), using 8 scans per FID and a total measurement time of 62 h. (b) 3D HN(CA)CB: spectrum was recorded as a $70^* \times 40^* \times 440^*$ data matrix with acquisitions times of 7.7 ms (t_1 , ^{13}C), 24 ms (t_2 , ^{15}N) and 54 ms (t_3 , ^1H), using 8 scans per FID and a total measurement time of 44 h. Complete assignments are listed in Table S1.

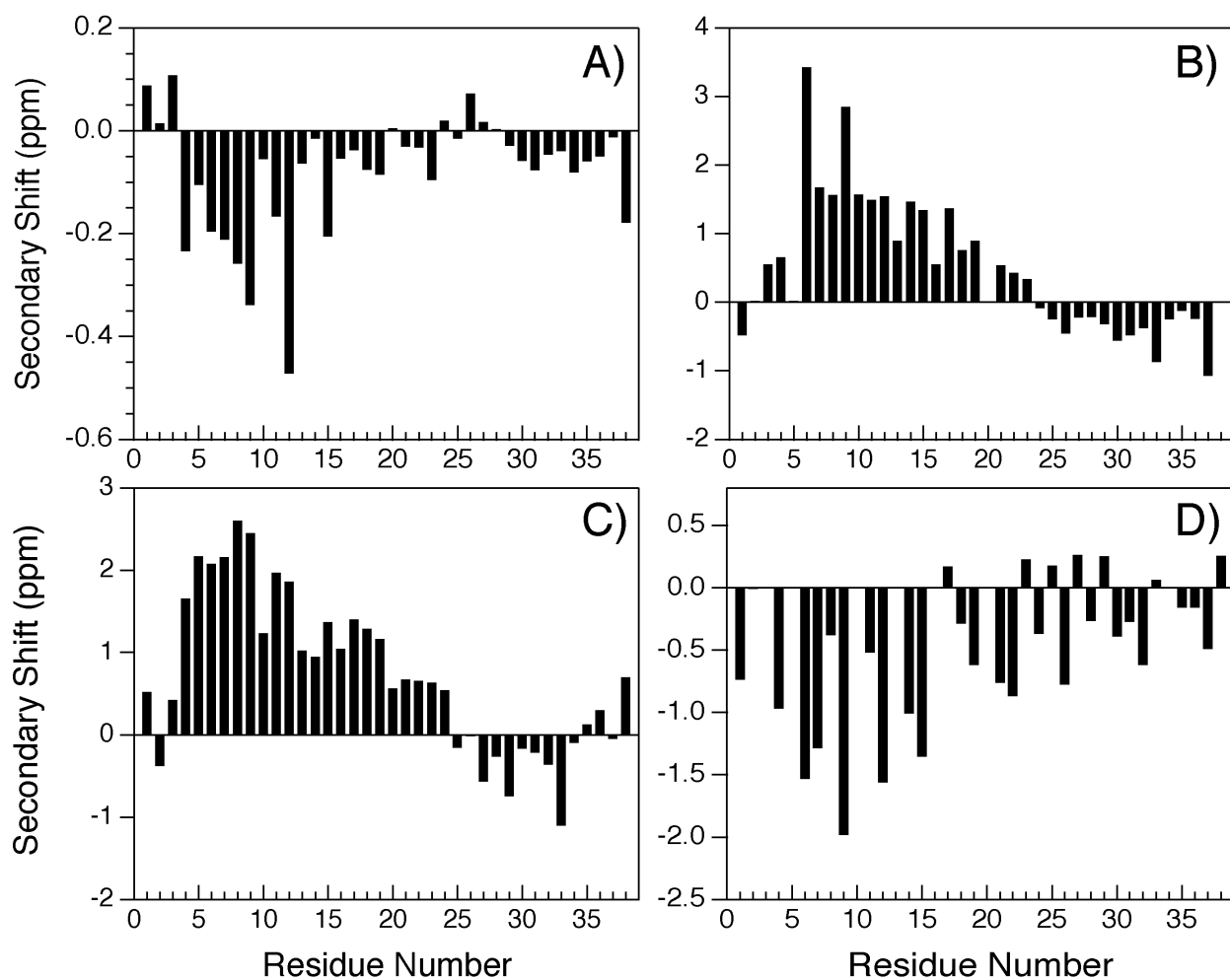


Figure S2. Secondary ^1H and ^{13}C chemical shifts for HIV-1 gp41 fusion domain. Secondary shifts ($\Delta\delta$) for $^1\text{H}^\alpha$ (a), $^{13}\text{C}^\gamma$ (b), $^{13}\text{C}^\alpha$ (c), and $^{13}\text{C}^\beta$ (d) were calculated as $\Delta\delta = \delta_{\text{EXP}} - \delta_{\text{RC}}$, where δ_{EXP} and δ_{RC} are the experimental and random coil chemical shifts (in ppm), respectively. The δ_{RC} values correspond to those used by the TALOS program (2).

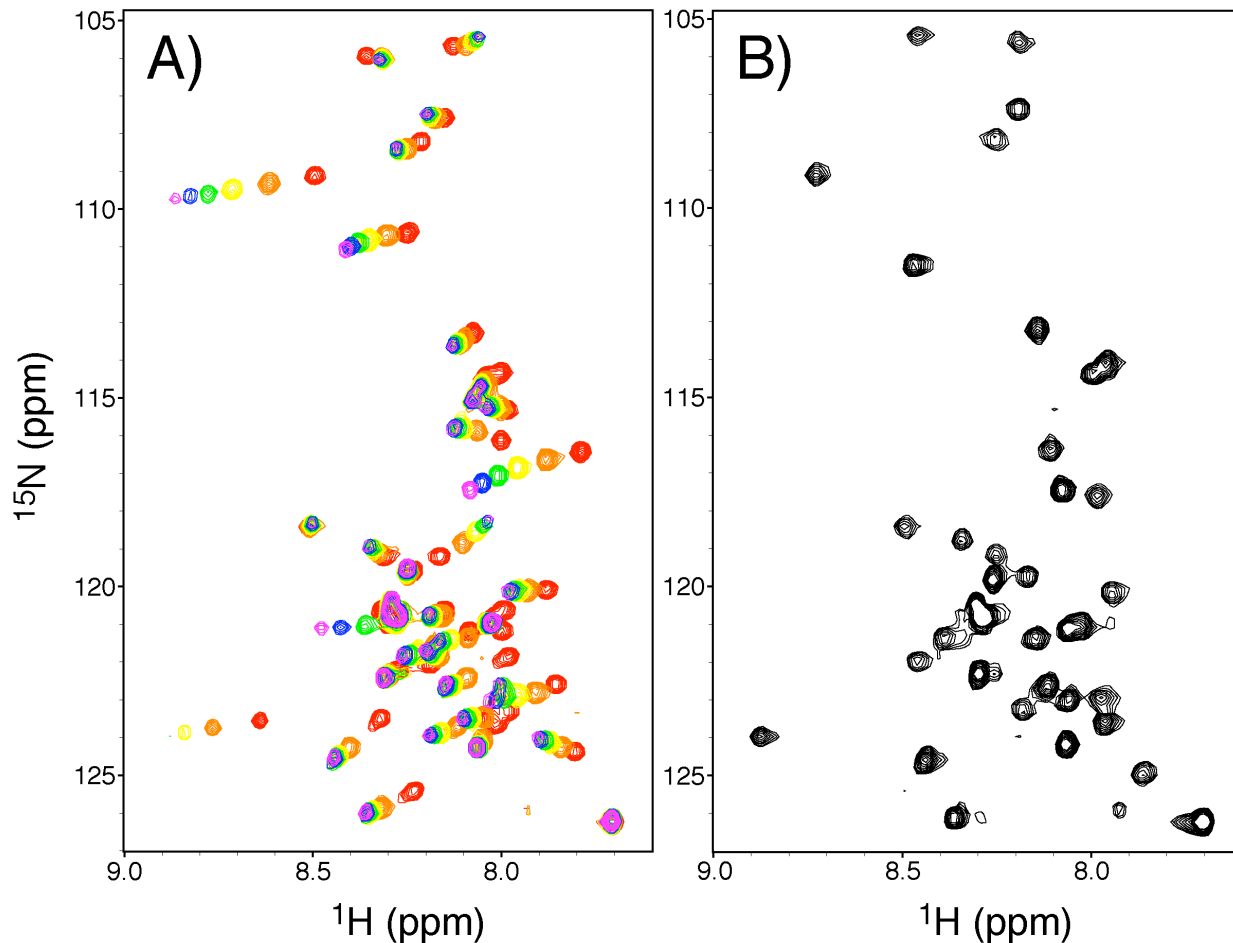


Figure S3. 750 MHz 2D ^{15}N - ^1H HSQC spectra of ^{15}N -labeled HIV-1 gp41 fusion domain in detergent micelles. (a) Spectra showing the titration of an initial 0.35 mM fusion peptide sample in 38 mM sodium dodecylsulfate (SDS) micelles with aliquots of 1 M solution of dodecylphosphocholine (DPC). The SDS:DPC concentrations in mM for the different samples are: 38:0 (red), 36:32 (orange), 35:62 (yellow), 34:91 (green), 33:118 (blue), and 32:143 (violet). (b) Spectrum of 0.35 mM fusion peptide in 100 mM 1-palmitoyl-2-hydroxy-sn-glycero-3-[phospho-RAC-(1-glycerol)] (LPPG) micelles. In addition to peptide and detergent, all samples contained 0.05% w/v NaN_3 , 7% D_2O , and 25 mM $\text{NaH}_2\text{PO}_4/\text{Na}_2\text{HPO}_4$ buffer to maintain a pH of 6.5. Spectra were recorded at 25 °C. The ^{15}N - ^1H HSQC spectra are very similar (majority of ^1H and ^{15}N chemical shifts are within 0.2 and 0.5 ppm, respectively, for different detergents; see also Figure S4) indicating that HIV-1 gp41 fusion domain adopts a similar structure in different membrane mimetics.

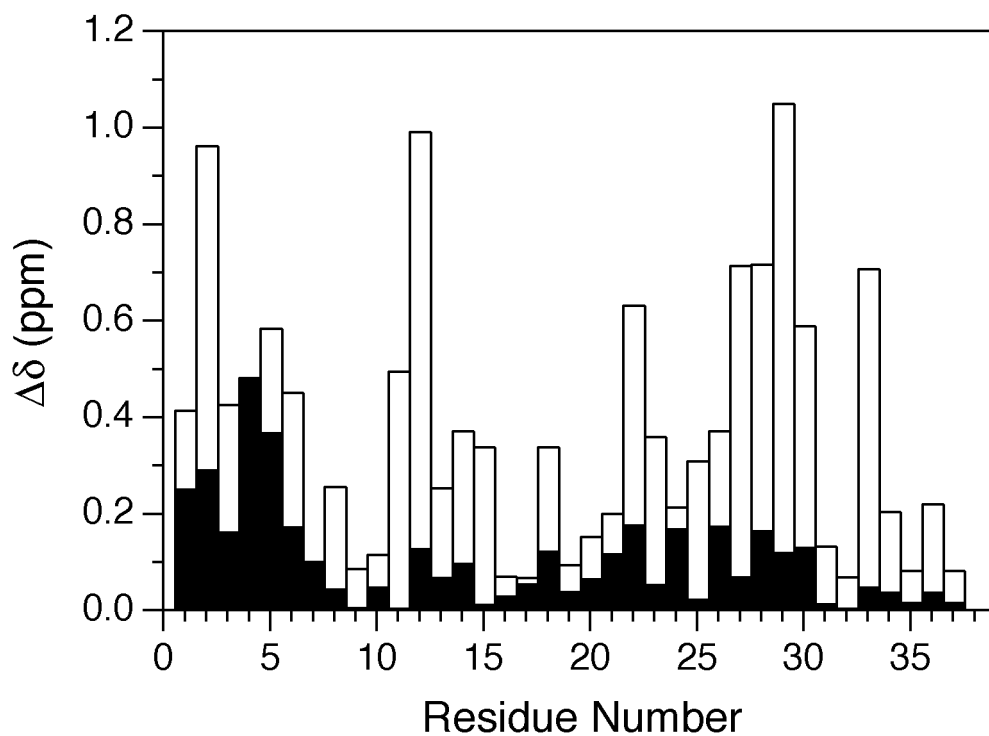


Figure S4. Absolute differences ($\Delta\delta$ in ppm) between amide ^1H (black) and ^{15}N (white) chemical shifts in 750 MHz 2D ^{15}N - ^1H HSQC spectra of ^{15}N -labeled HIV-1 gp41 fusion domain in SDS and mixed SDS/DPC micelles with the SDS:DPC ratio of 32:143 mM (*c.f.*, Figure S3). The majority of ^1H and ^{15}N chemical shifts are within 0.2 and 0.5 ppm, respectively.

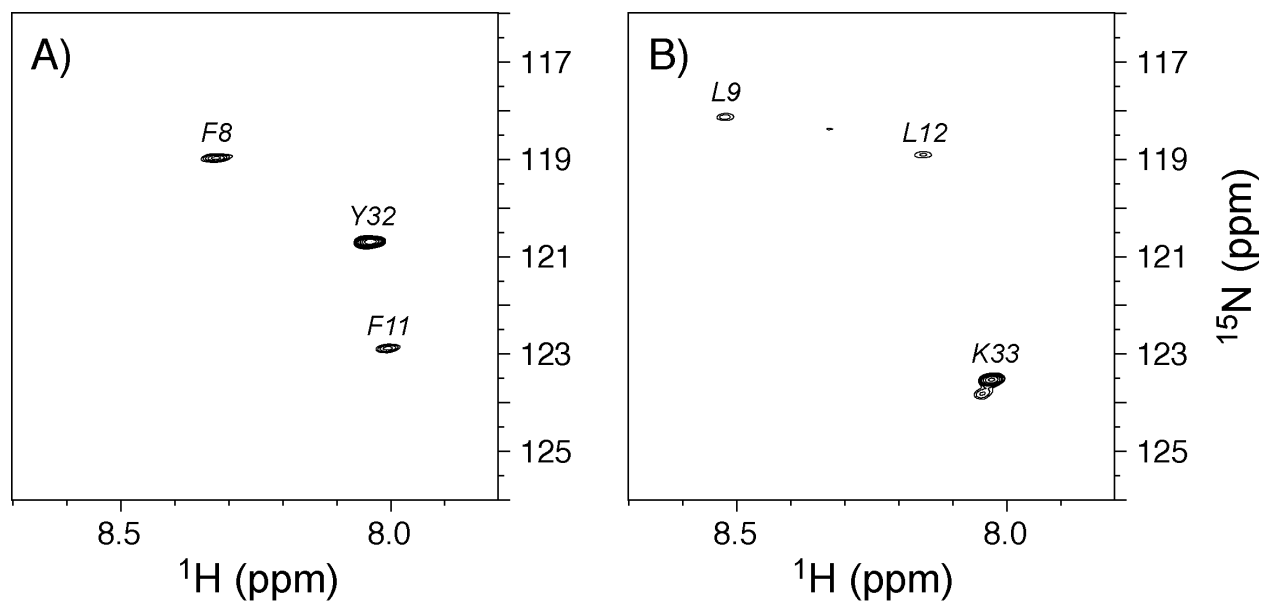


Figure S5. (a) 2D HNCG and (b) HN(CO)CG difference spectra for aromatic residues (Phe-8, Phe-11 and Tyr-32) of HIV-1 gp41 fusion domain. The spectra have been recorded using pulse schemes described in Hu et al. (3). The appearance of relatively intense cross-peaks in both difference spectra is indicative of χ^1 rotamer averaging for the aromatic residues, and the extracted $^3J_{\text{NC}_\gamma}$ and $^3J_{\text{C}_\gamma\text{C}_\beta}$ values are consistent with an approximately 1:1 ratio of the *trans* ($\chi^1 = 180^\circ$) and *gauche* ($\chi^1 = -60^\circ$) rotamers.

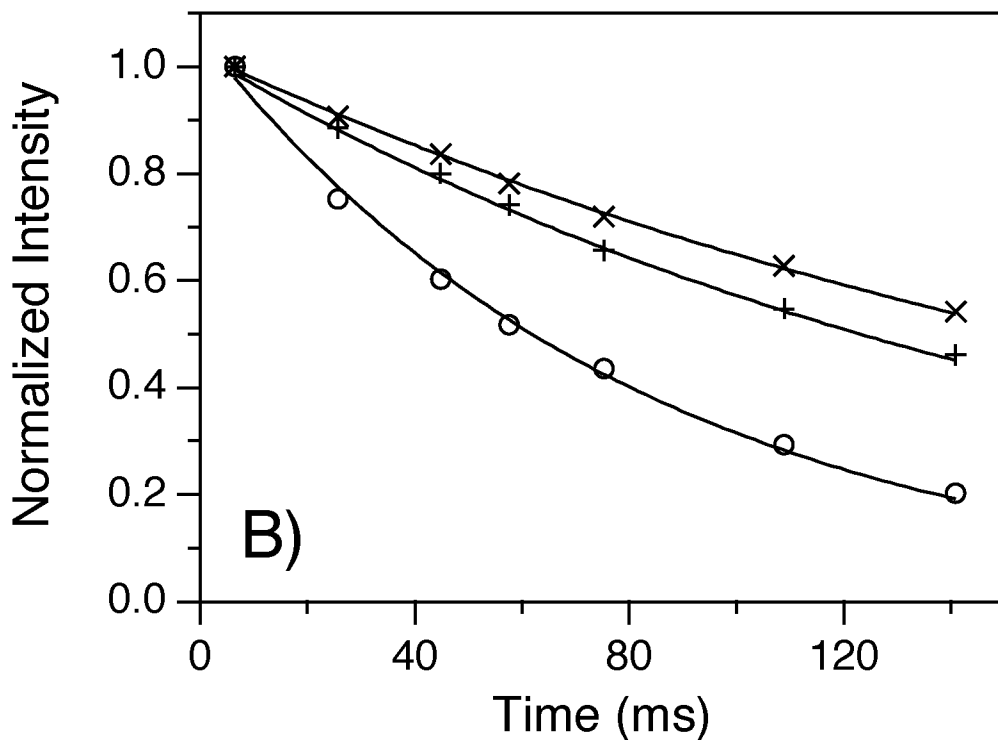
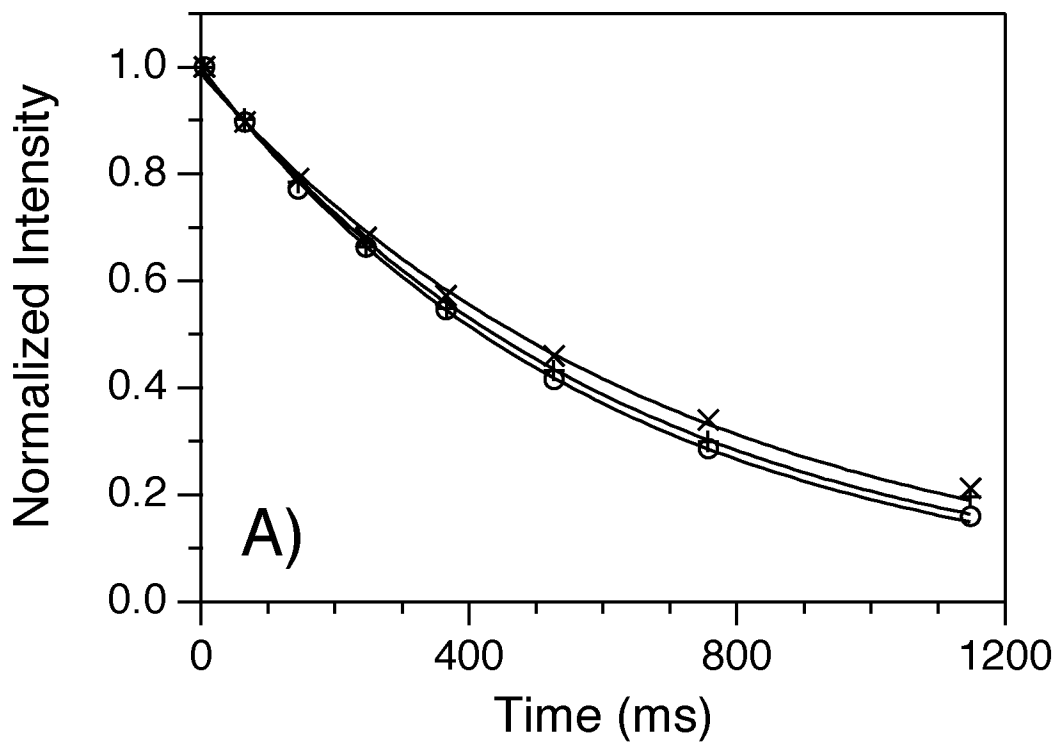


Figure S6. Representative T₁ (a) and T₂ (b) decay curves for the HIV-1 gp41 fusion domain. Shown are the data for residues Val-2 (x), Gly-10 (O) and Ser-23 (+). The solid lines indicate best fits to single exponential decays.

References

1. Yamazaki, T., Lee, W., Arrowsmith, C. H., Muhandiram, D. R., and Kay, L. E. (1994) A suite of triple resonance NMR experiments for the backbone assignment of ^{15}N , ^{13}C , ^2H labeled proteins with high sensitivity, *J. Am. Chem. Soc.* *116*, 11655-11666.
2. Cornilescu, G., Delaglio, F., and Bax, A. (1999) Protein backbone angle restraints from searching a database for chemical shift and sequence homology, *J. Biomol. NMR* *13*, 289-302.
3. Hu, J. S., Grzesiek, S., and Bax, A. (1997) Two-dimensional NMR methods for determining χ_1 angles of aromatic residues in proteins from three-bond $\text{JC}'\text{C}\gamma$ and $\text{JNC}\gamma$ couplings, *J. Am. Chem. Soc.* *119*, 1803-1804.